Stability of Complex Coacervate Core Micelles Containing Metal Coordination Polymer

ARTICLE *in* THE JOURNAL OF PHYSICAL CHEMISTRY B · OCTOBER 2008

Impact Factor: 3.3 · DOI: 10.1021/jp8044059 · Source: PubMed

Stability of Complex Coacervate Core Micelles Containing Metal Coordination Polymer

Yun Yan,*,† Arie de Keizer,† Martien A. Cohen Stuart,† Markus Drechsler,‡ and Nicolaas A. M. Besseling*,§

Laboratory of Physical Chemistry and Colloid Science, Wageningen University, Dreijenplein 6, 6703 HB Wageningen, The Netherlands, Makromolekulare Chemie II, University of Bayreuth, 95440 Bayreuth, Germany, Nano Structured Materials, Department of Chemical Engineering, Delft University of Technology, Julianalaan 136, 2628 BL Delft, The Netherlands

Received: May 19, 2008

We report on the stability of complex coacervate core micelles, i.e., C3Ms (or PIC, BIC micelles), containing metal coordination polymers. In aqueous solutions these micelles are formed between charged-neutral diblock copolymers and oppositely charged coordination polymers formed from metal ions and bisligand molecules. The influence of added salt, polymer concentration, and charge composition was investigated by using light scattering and cryo-TEM techniques. The scattering intensity decreases strongly with increasing salt concentration until a critical salt concentration beyond which no micelles exist. The critical micelle concentration increases almost exponentially with the salt concentration. From the scattering results it follows that the aggregation number decreases with the square root of the salt concentration, but the hydrodynamic radius remains constant or increases slightly. It was concluded that the density of the core decreases with increasing ionic strength. This is in agreement with theoretical predictions and is also confirmed by cryo-TEM measurements. A complete composition diagram was constructed based on the composition boundaries obtained from light scattering titrations.

Introduction

Polymeric micelles for which self-assembly is driven by electrostatic complexation between oppositely charged polyelectrolytes have recently received considerable attention, both because of their fundamental interest and in view of potential applications.[1−5] These micelles form spontaneously from oppositely charged polyelectrolytes in aqueous solutions, of which at least one is a charged-neutral block copolymer. Before mixing, none of the constituent components self-assembles in aqueous media. It is only upon mixing that complex coacervate cores are formed. These cores are protected from unlimited growth owing to the presence of the neutral block. Therefore, these micelles are denoted as "complex coacervate core micelles" (C3Ms),[6−8] "poly ion complex (PIC) micelles",[9,10] or "block ionomer complexes (BIC)".[3,11]

If one of the polyelectrolytes is substituted by some other charged species, C3Ms can be used for encapsulation of both "soft" materials, such as DNA and protein,[12,13] and "hard" nanoparticles such as oxide nanoparticles.[14,15] Recently, we found that the core can also be used as a nano carrier for metal ions when reversible metal coordination polymers are used as polyelectrolyte.[16,17] We have demonstrated the formation of quite monodisperse spherical micelles which consist of a diblock copolymer [poly(*N*-methyl-2-vinyl pyridinium iodide)-*b*-poly(ethylene oxide) ($P2MVP_{41}$-b-PEO_{205})] and a coordination polymer consisting of zinc ions connected by ditopic ligands [1,11-bis(2,6-dicarboxypyridin-4-yloxy)-3,6,9-trioxaundecane (L_2EO_4)].[18] The structure of the components is presented in Figure 1.

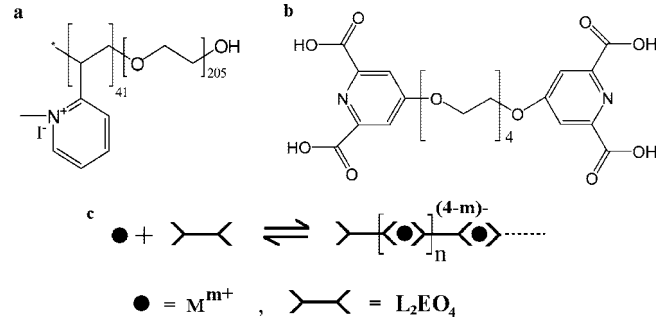

Figure 1. (a) Structure of $P2MVP_{41}$-b-PEO_{205}; (b) L_2EO_4; (c) illustration of a supramolecular coordination polymer.

When zinc ions are substituted by other metal ions, such as iron, cobalt, nickel, neodymium, lanthanum, holmium, or gold, micelles are also formed. This implies that a large range of metal ions can be carried by such micelles. This may find applications in delivery of functional ingredients in, e.g., medicine. Therefore, it is important to study the factors that determine the stability of these micelles.

Generally, C3Ms are stable in a narrow composition range around charge neutral mixing.[7,8,19] If the negative charge ratio f_- is defined as $f_- = [-]/([+] + [-])$, where $[-]$ and $[+]$ are the molar concentrations of negatively and positively chargeable groups, respectively, for each of the chains, stable C3Ms are usually formed around $f_- = 0.5$. This corresponds to a sharp increase of the scattered light intensity around this composition as schematically shown in Figure 2a. Outside this region only small soluble complexes (SC) exist which scatter weakly. In a plot of the concentration of the cationic component against that

* To whom correspondence should be addressed. E-mail: yun.yan@wur.nl (Y.Y.); N.A.M.Besseling@tudelft.nl (N.A.M.B.). Current address for Y. Y.: College of Chemistry and Molecular Engineering, Peking University, Beijing 100871, China. E-mail: yunyan@pku.edu.cn.

† Wageningen University.

‡ University of Bayreuth.

§ Delft University of Technology.

10.1021/jp8044059 CCC: $40.75
Published on Web 08/12/2008

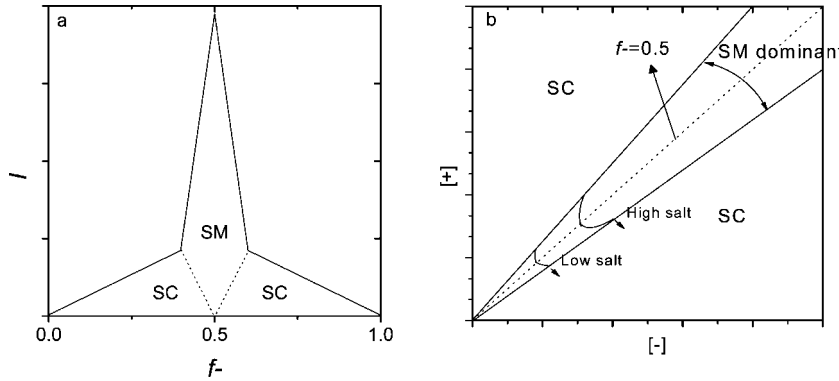

Figure 2. (a) Typical light scattering diagram of C3Ms.[7] The scattered intensity *I* is plotted against the negative charge fraction *f*-. (b) Schematic composition diagram of the same system. SC: soluble complexes; SM: spherical micelles.

of the anionic component (Figure 2b), one can find a region which is dominated by spherical micelles (SM) around the line of $f- = 0.5$. Strictly speaking, only at $f- = 0.5$ can we expect pure SM; off the $f- = 0.5$ line a small amount of SC should be present as well. That is why we denote the SM region as SM dominant in Figure 2b.

As should be expected, ionic strength affects the stability of C3Ms, since micelle formation is driven by electrostatic interaction. Indeed, it has been reported that PIC micelles disintegrate at a certain salt concentration due to shielding of charges on the polyelectrolyte chains.[20−22] However, for the new class of C3Ms containing metal-coordination polymers such information is still missing.

In our studies on metal-containing C3Ms so far, we observed that, depending on the composition, different self-assembled objects are formed: 'true', rather monodisperse spherical micelles,[16] soluble complexes, and also in some cases a combination of spherical micelles and large worm-like micelles.[23] Here we intend to map out the regime where the spherical micelles are stable, both with respect to dilution, composition, and ionic strength. In this study, the coordination polymer Zn-L_2EO_4 was prepared at a 1:1 molar ratio, i.e., $[Zn^{2+}] = [L_2EO_4]$. The micellar stability against *f*-, dilution, and addition of indifferent salt (NaCl) was studied. The critical micellar concentrations at various salt concentrations were measured, and a "composition diagram" which figures out the region for different stable species was constructed.

Experimental Section

1. Materials. The diblock copolymer used in this study, poly(*N*-methyl-2-vinyl-pyridinium iodide)-*b*-poly(ethylene oxide) ($P2MVP_{41}$-b-PEO_{205}), was obtained by quaternization of poly(2-vinylpyridine)-*b*-poly(ethylene oxide) ($P2VP_{41}$-b-PEO_{205}) (Polymer Source, $M_w/M_n = 1.03$, $M_w = 13.3$ k) following a procedure described elsewhere.[24] The degree of quaternization is about 90%.[25] Each quaternized 2-vinyl pyridinine carries one positive elementary charge.

The bisligand compound 1,11-bis(2,6-dicarboxypyridin-4-yloxy)-3,6,9-trioxaundecane (L_2EO_4) was prepared according to literature.[14,26] Piperazinebis(ethanesulfonic acid) (PIPES, 98%) was obtained from Aldrich. Sodium hydroxide (NaOH) and zinc nitrate ($Zn(NO_3)_2 \cdot 6H_2O$) were analytical grade. Zn-L_2EO_4 coordination polymer was prepared by mixing solutions of $Zn(NO_3)_2 \cdot 6H_2O$ and L_2EO_4 at 1:1 molar ratio in 20 mM PIPES-NaOH buffer. Each coordination center of Zn-L_2EO_4 carries two negative charges, therefore, the negative charge concentrations for the Zn-L_2EO_4 coordination polymer equals twice the concentration of Zn or L_2EO_4 at $[Zn] = [L_2EO_4]$. Ultrapure water was used throughout the experiments. All solutions were prepared in the same PIPES-NaOH buffer at pH 5.4.

2. Methods. ***2.1. Laser Light Scattering (LLS).*** Light scattering (LS) measurements were performed with an ALV laser light scattering apparatus, equipped with a 400 mW argon ion laser operating at a wavelength of 514.5 nm. A refractive index matching bath of filtered *cis*-decalin surrounded the cylindrical scattering cell, and the temperature was kept constant at 25 °C within ±0.5 °C using a Haake C35-F8 thermostat. The laser light scattering intensity at 90° and the intensity auto correlation function were recorded. The data were analyzed both by the CUMULANT and the CONTIN method.

2.1.1. Determination of the Critical Micellar Concentration (CMC) at Low Ionic Strength. A concentrated dust-free micellar solution at $f- = 0.5$ was prepared in 20 mM buffer, then the solution was diluted step by step with dust-free 20 mM PIPES buffer. After each dilution, the scattered light intensity at 90° was measured. The scattered light intensity (*I*) against polymer concentration expressed in terms of the molar concentration of chargeable groups ($[+] = [-]$) was plotted. Extrapolation of the curve to zero scattering was made, and the polymer concentration with a zero scattering intensity was taken as CMC.

2.1.2. Determination of the Effect of Salt on the CMC. Stock dust-free micellar solutions at $f- = 0.5$ in 20 mM PIPES buffer were prepared with and without 300 mM NaCl. Two solutions of the same concentration, but with and without NaCl, were mixed at different ratios to obtain solutions of different NaCl concentration. In the plot of *I* against the NaCl concentration, the salt concentration at the break point was established for a particular micellar concentration. Plotting the polymer concentration ($[+] = [-]$) against the salt concentration at the break points (C_s) gives the dependence of the CMC upon the salt concentration.

2.2. Cryogenic Transmission Electronic Microscopy (Cryo-TEM). A few microliters of sample were placed on a bare copper TEM grid (Plano, 600 mesh), and the excess liquid was removed with filter paper. This sample was cryo-fixed by rapidly immersing into liquid ethane cooled to −170 to −180 °C in a cryo-box (Carl Zeiss NTS GmbH). The specimen was inserted into a cryo-transfer holder (CT3500, Gatan, Munich, Germany) and transferred to a Zeiss electron microscope EM922 EFTEM (Zeiss NTS GmbH, Oberkochen, Germany). Examinations were carried out at temperatures around −180 °C. The TEM was operated at an acceleration voltage of 200 kV. Zero-loss filtered images were taken under reduced dose conditions (500−2000 e/nm^2). All images were recorded digitally by a bottom-mounted CCD camera system (UltraScan 1000, Gatan) and processed

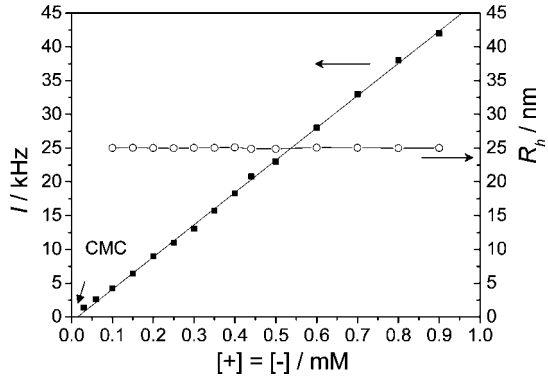

Figure 3. Scattered light intensity (I, solid squares) and mean hydrodynamic radius (R_h, open circles) versus polymer concentration in the micellar system at $f\text{-} = 0.5$. The markers are experimental data and the solid lines are linear fits. The CMC value in 20 mM PIPES buffer was obtained by extrapolation of the scattering line to zero scattering.

with a digital imaging processing system (Digital Micrograph 3.9 for GMS 1.4, Gatan).

2.3. Composition Diagram. The composition boundaries were determined by light scattering titrations as described elsewhere.[17] The experiments were performed with an ALV laser light scattering apparatus, equipped with a 400 mW argon ion laser operating at a wavelength of 514.5 nm. The scattered light intensities vary with the fraction of the negative charges, $f\text{-}$. The $f\text{-}$ at which the scattered light intensity starts to increase is taken as the start of formation of micelles. All the scattered intensities were recorded at a scattering angle of 90°.

Results and Discussion

1. CMC of the Micellar System at Low Polyelectrolyte Concentration. It was reported that C3Ms show a critical association behavior,[20,27,28] which is similar to that for block copolymer micelles formed through the different solubility of the constituent segments in selective solvents. Analogously to surfactant systems, this concentration may also be called a critical micelle concentration (CMC). One should bear in mind that some authors have used the term *critical aggregation concentration* (CAC).[21,27] Considering the similarity to conventional surfactants, we prefer to use CMC here. For many practical (medical) applications, systems are inevitably diluted, and therefore, the value of the CMC is very relevant. When speaking of CMC in this work, the micelles referred to are those formed at exact charge neutral mixing ratio, i.e., $f\text{-} = 0.5$. The CMC will strongly depend on salt concentration. In this section, we will consider the CMC at $f\text{-} = 0.5$ in the presence of 20 mM buffer but without other added salt.

Figure 3 demonstrates the variation of the scattered light intensity with concentration. The scattered light intensity decreases linearly with dilution. The linearity is still valid even down to 0.03 mM, indicating that micelles are still present at extremely low concentrations. Their size remains constant upon dilution. This is confirmed by the CUMULANT hydrodynamic radii also shown in Figure 3. The above results indicate that the CMC of the C3Ms are lower than 0.03 mM, which agrees well with Kataoka's result that the CAC of their PIC micelles is very low.[27] By extrapolation to zero scattering, we obtain a value for the CMC $\approx$ 0.02 mM. The actual value will be slightly higher due to neglect of the scattering of polymers from decomposed micelles, but it will still be below 0.03 mM. This value is sufficiently low for practical applications. Such a low decomposition concentration indicates that the micelles have a strong ability to resist dilution within 20 mM PIPES buffer.

2. Stability and Aggregation Number of Micelles in the Presence of NaCl. Stability of micelles under physiological conditions is of much interest for potential biomedical applications. Therefore, we also investigated the micellar behavior in the presence of added salt. Both LLS and cryo-TEM experiments were carried out for this system.

2.1. Influence of NaCl on the Scattering Intensity and Micellar Size. In Figure 4a we present the light scattering intensity as a function of the NaCl concentration for four dilute solutions (0.22∼0.76 mM) and one concentrated one (1.77 mM) of Zn-L_2EO_4/P2MVP_{41}−PEO_{205} at $f\text{-} = 0.5$. The radii for the mixed solutions of 0.76 (solid triangles) and 1.77 mM (solid squares) are presented in Figure 4b. Radii for the other three lower concentrations could not be accurately determined due to the low scattered intensity. Note that neither the PIPES buffer (20 mM) nor any counterions released during formation of micelles are included in the NaCl concentration on the abscissa of Figure 4.

As can be seen from Figure 4a for all four micellar systems with low concentrations the scattered light intensities decrease almost linearly with increasing NaCl concentration and level off at a critical value. For solutions at higher polymer concentration, a sharp increase of the scattered light intensity was observed following the original linear decrease. As the scattered light intensity approaches a maximum, longer time is required for the system to get a stable intensity (data not shown). The intensities presented in Figure 4a are the equilibrium values which remain stable in time. It is also noted that, in the low [NaCl] regime, the scattered light intensity decreases also linearly with the polymer concentration at fixed [NaCl] (Figure 4a, inset), which is similar to that observed in the absence of NaCl (Figure 3). CUMULANT radii for these solutions indicate that, in the linear regime, the mean hydrodynamic radius of the micelles is constant, but it tends to increase close to the critical NaCl concentration. This tendency is more pronounced for concentrated solutions, as shown in Figure 4b, which shows a considerable increase of the micellar size with increasing NaCl concentration. Similar to the scattering intensities, the hydrodynamic radii are also equilibrium values that remain stable in time. According to literature, the influence of added salt on C3Ms is very complicated.[20−22] Depending on the nature of the system, the decrease of the scattered light intensity can be linear,[20,22] parabolic, [20] or a linearity followed by a sharp increase.[21] In the present situation, the micellar size as probed by DLS remains constant in low salt concentration but gradually increases at higher salt concentration. According to a theoretical prediction by Kramarenko et al.,[29] the aggregation number of the micelles will decrease upon addition of NaCl as a consequence of a decrease of the volume fraction of the polymers in the micellar core. It has been argued that the disintegration of PIC micelles is due to the screening effect of the added salt. Therefore, one would expect that the aggregation number depends linearly on the square root of the total salt concentration. However, no experimental data have been reported for this relationship. Recalling our LS results, the micellar mass and the scattered light intensity can be related to each other by the following equation:

$$(I - I_0) \propto CM = Cnm_{bb} = (C_t - \mathrm{CMC})nm_{bb} \qquad (1)$$

where I is the apparent scattering intensity observed directly for the whole system, I_0 is the scattering intensity from the unimer solution, C is the weight concentration of the micelles

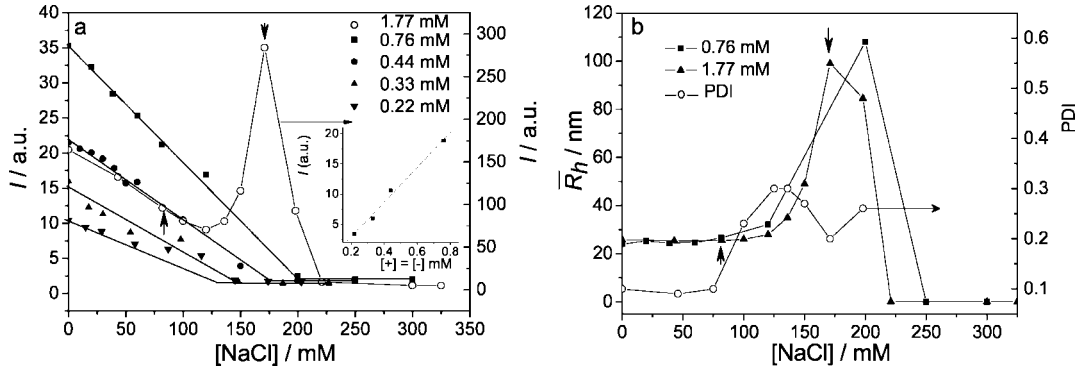

Figure 4. (a) Variation of the scattered light intensity for micellar systems of different concentrations with increasing [NaCl]. The scale for the 1.77 mM system is given in the right axis. The inset is the variation of the scattered light intensity with polymer concentration at 100 mM NaCl. (b) Variation of the mean hydrodynamic radius for the [+] = [−] = 0.76 (solid squares) and 1.77 (solid triangles) mM systems with increasing [NaCl]. The change in the CUMULANT polydispersity index for the 1.77 mM system (PDI, open circles) is also shown in this figure.

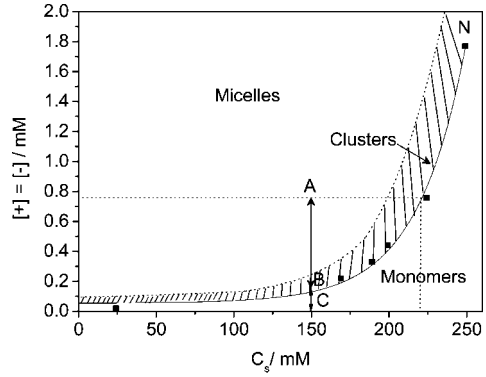

Figure 5. CMC curve (solid curve across solid squares) of the micelles in the presence of added salt. The dashed area is to illustrate quantitatively the region where clusters are present. Notice that here the PIPES buffer and the counterions were taken into account in C_s. The PIPES buffer at pH 5.4 is viewed as 1−1 type electrolyte. T = 25 °C.

in the solution, M is the weight of one micelle, n is the aggregation number, m_{bb} is the weight of a building block (that is,the molecular weight of the cationic block polymer plus the stoichiometric amount of coordination polymer) that forms micelles, C_t is the total weight concentration of polymers, and CMC is the critical micelle concentration in the presence of salt, which will be further discussed below. As m_{bb} is constant for a given system, the reduced scattering intensity $(I - I_0)/(C_t - \mathrm{CMC})$ is proportional to the aggregation number n. The relation between $(I - I_0)/(C_t - \mathrm{CMC})$ and the square root of the total salt concentration $\sqrt{C_s}$ will be discussed in detail in the following text. For this purpose, we first present the influence of the added salt on CMC.

2.2. Influence of Salt on CMC. The CMC of C3Ms are very sensitive to the presence of salt. In the present system, the salt to be considered includes the added NaCl, the PIPES buffer ions, and the counterions released to the bulk solution upon formation of C3Ms. Therefore, C_s in the following text is the sum of the NaCl concentration, the concentration of the buffer (equivalent to 20 mM NaCl, since it can be considered approximately as 1−1 type electrolyte at pH 5.4 due to 50% dissociation), and the free ions released upon formation of micelles.

The polymer concentration versus the total salt concentration C_s at the breaking points in Figure 4a can be used to map out the region where micelles exist (Figure 5, solid squares). The solid curve drawn in Figure 5 (fit to solid squares) can then be viewed as the dependence of the CMC on added salt. Below this curve, no micelles are formed and the polymers are present as unimers or in small soluble complexes; whereas above this curve, micelles dominate. It should be kept in mind that close to the critical salt concentration, there is a region in which irregular clusters—instead of well-defined micelles—dominate, as roughly estimated by the dashed area in Figure 5.

We find, in Figure 5, that the CMC increases exponentially with the concentration of NaCl in the low concentration regime. Obviously this is opposite to the behaviors of ionic surfactant systems. Salt shields the headgroup charges of ionic surfactant molecules, which decreases the repulsion between surfactant molecules. This facilitates micelle formation. Therefore, addition of salt decreases the CMC of an ionic surfactant. In the case of C3Ms, electrostatic attraction is the main driving force for formation of micelles; addition of salt will weaken this interaction by shielding of charges. Therefore, addition of salt disfavors C3M formation.

The experimental data can be fitted by an exponential relation between the CMC and the concentration of NaCl:

$$\mathrm{CMC} = 0.056 + 0.00064 \exp(C_s/31.52) \qquad (2)$$

where both the CMC and C_s are expressed in millimolar. From this relation, one can easily obtain not only the CMC at a given salt concentration but also the ratio between micelles and unimers or small soluble complexes at any given salt concentration. For instance, for the 0.76 mM micellar system, the amount of unimers and small soluble complexes can be read in Figure 5 from the length of arrow **BC**, whereas the materials in the micelles are expressed by the length of arrow **AB**. With such a regulation, we can easily determine what concentration should be prepared in terms of application. The qualitative relation between the CMC value and salt concentration allows us to predict the required polymer concentration in a physiological environment. Of course, due to the influence of added salt on the micellar structures, it is better to avoid a concentration that is close to these CMCs.

2.3. Influence of Salt on the Aggregation Number. Using the relation for the salt dependence of CMC given by eq 2, we can replot Figure 4a using the reduced scattering intensity $(I - I_0)/(C_t - \mathrm{CMC})$, which is proportional to the aggregation number n according to eq 1. As electrostatic screening is usually proportional to the Debye length, that is, to the square root of salt concentration, we accordingly present the reduced scattering intensity in Figure 4a against the square root of the total salt concentration C_s in Figure 6. The data in Figure 6 are collected at salt concentrations in the original linear region which are lower than the break points in Figure 4a.

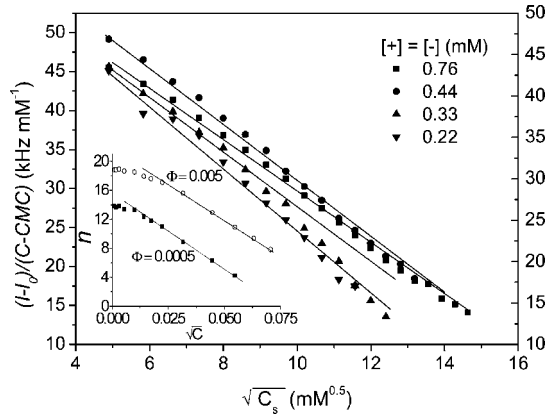

Figure 6. Variation of $(I - I_0)/(C_t - \mathrm{CMC})$ which is proportional to the micellar aggregation number with the square root of the total salt concentration C_s. Counterions released upon formation of micelles and the PIPES buffer are included in C_s. The polymer concentrations are as follows: 0.76 mM, solid squares; 0.44 mM, solid circles; 0.33 mM, solid upward triangles; 0.22 mM, solid downward triangles. The lines are guidance for linearity. The inset is the theoretical result of Kramarenko et al. The data were read from ref 27, Figure 7, and replotted here. These data were collected for salt concentrations lower than the break points. This inset illustrates the variation of the aggregation number n against the square root of salt concentration $\sqrt{C_s}$ for two different polymer concentrations, e.g., for the polymer volume fraction of $\Phi = 0.0005$ and 0.005, respectively.

Figure 6 clearly illustrates that data from the linear region in Figure a, replotted as $(I - I_0)/(C - \mathrm{CMC})$ vs $\sqrt{C_s}$ produce a linear relation for the considered systems, which indicates that the disintegration of micelles is indeed due to the shielding of charges on the polyions by the added inorganic salt. Moreover, the lines for various polymer concentrations are very close, suggesting that the relation between the aggregation number n and $\sqrt{C_s}$ is unique. The data quality for the 0.22 and 0.33 mM systems is not as good as that for 0.44 and 0.76 systems, which might be a result of bigger error for low concentrations. These results agree well with the theoretical prediction by Kramarenko et al.,[29] as shown as the inset in Figure 6. It is clear that at medium salt concentration, the theoretical aggregation number n decreases linearly with the square root of salt concentration.

It is also noticed in the inset that at very low salt concentration, the aggregation number is hardly influenced by the presence of salt, as is not observed in our experimental results. This is probably because the salt concentration we start working with is not low enough. It is understandable that at very low salt concentrations shielding hardly occurs. Another feature in the inset is the concentration dependent aggregation number from the theoretical prediction. It reveals that aggregation number increases slightly with polymer concentration. Read from the inset in Figure 6, as the polymer concentration is decreased by one order, the aggregation number is decreased only by about 35%. The slow decrease of the aggregation number with decreasing polymer concentration perhaps explains our experimental results that the aggregation number seems unique in the concentration range 0.2∼0.8 mM. Combining theoretical and experimental results, we can unambiguously conclude that the disintegration of the C3Ms or PIC or BIC complex upon addition of salt is indeed due to electrostatic screening.

The electrostatic screening causes the decrease of the aggregation number; meanwhile, the number of micelles increases. This can be inferred from eq 1. Surprisingly, the decrease of the aggregation number does not result in a corresponding decrease of the micellar size as measured by the hydrodynamic

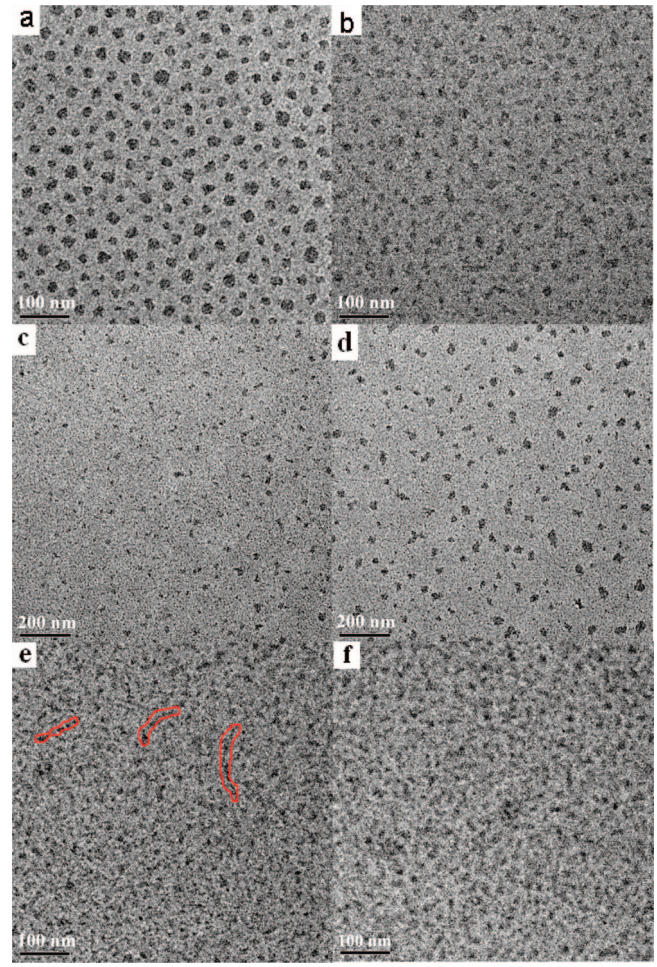

Figure 7. Cryo-TEM images of the mixed solutions of 1.77 mM $P2MVP_{41}$-b-PEO_{205}/Zn-L_2EO_4 at f- = 0.5: (a) no NaCl; (b−d) 80 mM NaCl; (e, f) 170 mM NaCl.

radius (Figure 4b); instead we find a constant or weakly increasing size. This must imply that the micelles swell upon addition of NaCl. According to the theory of Kramarenko et al., the core−corona interfacial tension decreases with salt concentration, which will indeed result in swelling of the micellar core.[29] However, such results have not been directly confirmed experimentally yet. Some DLS results show, like ours, a constant or slight increase of the hydrodynamic radius of micelles upon increasing salt concentration.[21,30] But DLS alone cannot provide information about the micellar core. For this, intensity data are critical. For our micellar system, we can probe the salt effects by an added experiment. The presence of metal ions allows us to use transmission electron microscopy (TEM) to observe the core directly. In the following we will present the cryo-TEM investigation about the morphology of the micelles upon addition of NaCl.

3. Influence of NaCl on the Morphology of the Micelles. In Figure 7 we show the cryo-TEM results for the 1.77 mM micellar system at various NaCl concentrations. For comparison, the image with no added NaCl is also presented (Figure 7a). In the case of no added salt, well-defined micelles with high contrast are clearly visualized everywhere owing to the presence of zinc ions in the coacervate cores. This appearance is independent of polymer concentration.[16] In contrast, upon addition of 80 mM NaCl (this is the range where the scattering intensity I is decreasing linearly with increasing [NaCl] but the micellar hydrodynamic radius (R_h) remains unchanged as indicated by the upward arrows in Figure 4a,b), the morphology

of the micelles shows diversity to some degree. On one hand, ill-defined micelles of poor contrast appear in this sample (Figure 7b); on the other hand, rather polydisperse particles of good contrast but with irregular shapes also exist in the same sample (Figure 7c,d). Both observations indicate that the structure of the micelles has been affected by the presence of added salt, although their *average* hydrodynamic radius obtained by DLS appears unchanged. The particles with poor contrast and much smaller size no doubt have less polymer in the core, which agrees well with the theoretical prediction that a low volume fraction of polymers is present in the core at high salt concentration.[29] The larger irregular particles found in the same solution are probably rearranged structures caused by the decrease of the core−corona interfacial tension, which may be related to the change of molecular packing parameter p as will be discussed later. The diversity in micellar size upon addition of NaCl is also in good agreement with the high PDI under the same conditions as showed in Figure 4b (open circles). A similar decrease of the scattering intensity upon addition of NaCl accompanied with a constant hydrodynamic radius was also observed by other groups using DLS.[21,30] However, they concluded from the constant hydrodynamic radius that the micellar structure remains unchanged upon addition of NaCl.[21] According to our Cryo-TEM result, this is, at least for our system, obviously not the case. Further static light scattering measurements would be desired to measure the aggregation number in greater detail, in order to better understand the structural change of the micelles upon addition of salt.

At very high salt concentration (170 mM, Figure 7e), where both the scattered light intensity and the CUMULANT particle sizes show a maximum (downward arrows in Figure 4 a,b), the cryo-TEM results indicate the existence of ill-defined, large polymeric clusters. These clusters exist either in the form of long worms (see structures enclosed by red lines in Figure 7e) or irregularly shaped particles (of which we observe many in Figure 7e,f). Obviously, the strong scattering comes from these big clusters. Observation of large clusters close to the critical salt concentration is a common phenomenon for C3Ms.[21] The advantage of our C3Ms containing metal coordination polymer is that these structures can be conveniently observed by TEM owing to the presence of electron-rich metal ions. To our knowledge, this is the first time that these large irregular clusters are seen directly. It is noteworthy in Figure 4b that the PDI for the optimal clusters shows a minimum at [NaCl] = 170 mM, which indicates that clusters of similar structure and size are formed predominately everywhere at this [NaCl]. This is really the case in the cryo-TEM results as shown in Figure 7e,f. Large clusters seem to fill the image, and the sizes are more homogeneous than for the 80 mM NaCl situation.

These dominating cluster structures are probably caused by an increased molecular packing parameter. According to Israelachvili,[31] the molecular packing parameter p for a self-assembling amphiphile systems is defined as $p = v_0/al$, where v_0 is the volume of the hydrophobic chain of an amphiphile molecule, a is the area of the amphiphile's headgroup at the water−aggregate interface, and l is the length of the hydrophobic tail. Small p ($p < 1/3$) favors structures with large curvature, such as spherical micelles. Increasing p leads to formation of rods and bilayered structures which have smaller curvature. For a given amphiphilic molecule, v_0 and l are fixed, so that p can be modified by changing environmental conditions because the value of a responds to temperature, salt concentration, electrostatic interaction, etc.[32,33] For a complex coacervate system, one pair of oppositely charged polyelectrolyte chains can be considered as a 'hydrophobic chain' having a volume v_0. However, in this case, v_0 also becomes environmental responsive because it is related with electrostatic interaction. Upon addition of salt, the screening effect between the pair of oppositely charged polyelectrolytes weakens the attraction. As a consequence, the pair has to swell, i.e., v_0 increases. The swelling of the oppositely charged pair also results in an increase of a. In this case, the change of p is determined by the ratio of v_0/a (l remains unaffected by addition of salt). Because v_0 and a are proportional to the cubic and square of the distance between the oppositely charged polyelectrolyte pair, respectively, an increase in v_0 is therefore always larger than increase in a. As a result, p increases upon addition of salt. This suggests that structures with large curvature will be formed upon addition of [NaCl]. The large clusters observed in cryo-TEM are therefore probably such structures.

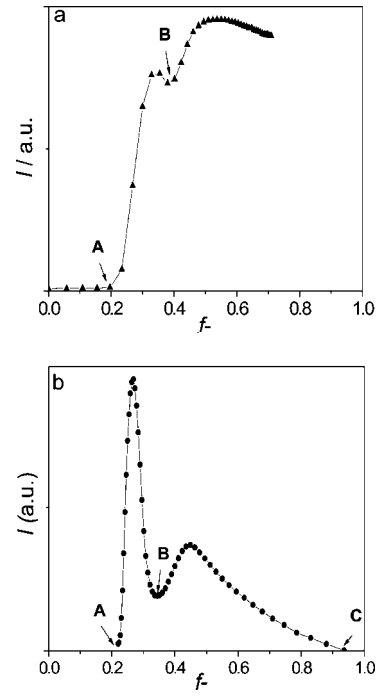

Figure 8. Light scattering titration of (a) 0.88 mM $P2MVP_{41}$-b-PEO_{205} solution with 2.3 mM Zn-(L_2EO_4) coordination polymer; (b) 0.87 mM Zn-(L_2EO_4) with 4.34 mM $P2MVP_{41}$-b-PEO_{205} solution. Arrows **A** and **B** indicate the range where worm-like micelles occur; **B** and **C** indicate the range of 'pure' spherical micelles. Spherical micelles actually exist in the whole range between **A** and **C**. $T = 25$ °C; 20 mM PIPES buffer.

4. Composition Diagram. Up to now, we considered the effect of NaCl on the stability of the micelles at $f- = 0.5$ in the mixed system of $P2MVP_{41}$-b-PEO_{205}/Zn-(L_2EO_4). We now combine these results with the micellar composition boundaries at excess positive or negative charges to obtain a complete "composition diagram" of our $P2MVP_{41}$-b-PEO_{205}/Zn-(L_2EO_4) mixed system. The composition boundaries were obtained by titration of $P2MVP_{41}$-b-PEO_{205} to Zn-(L_2EO_4) solution of different concentrations. Typical results are plotted in Figure 8.[23] The micellar boundaries follow from the $f-$ values where the intensity starts to increase or decrease.

For example, between **A** and **B** are worm-like micelles (WM); between **B** and **C** are 'pure' spheres, i.e., without worms. We know from previous cryo-TEM results that worm-like micelles always coexist with spherical ones;[23] therefore, the spherical micelles actually cover the worm-like micellar region, but there is a boundary between the pure spherical micelles and the mixture of spherical and worm-like ones, as shown in Figure 9.

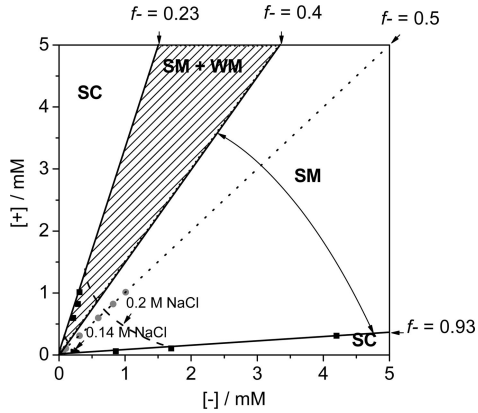

Figure 9. Composition diagram for the Zn-L_2EO_4/P2MVP$_{41}$−PEO$_{205}$ mixed system: SC, soluble complexes; SM, spherical micelles; WM, worm-like micelles. The solid line represents the composition boundaries. The markers (solid squares and circles) are the experimental data. The gray area is the region where SM and WM coexist. The dotted line across the red circles has $f- = 0.5$, i.e., along this line, the concentration of negative charges and positive charges is equal and formation of micelles is optimal. The two convex dashed lines designate the composition boundary when indifferent salt is added.

As can be read from Figure 9, spherical micelles (SM) exist in a broad *f*- region between $f- = 0.23$ and 0.93. Outside this region, only soluble complexes (SC) are formed. There is a narrow region between $f- = 0.23$ and 0.4 in which spherical micelles and worm-like micelles coexist (SM + WM). We reported the existence of worm-like micelles in our previous work.[23] Added evidence from small-angle X-ray scattering will be published shortly. Between $f- = 0.4$ and 0.93, there is a rather wide regime composed of only narrowly distributed spherical micelles. This result may be relevant to applications. In addition, indifferent salt, e.g., NaCl, affects the concentration at which the micelles starts to form. The higher the NaCl concentration, the higher the Zn-L_2EO_4/P2MVP$_{41}$−PEO$_{205}$ concentration it requires. We expect that several general features in Figures 6 and 9 are common for C3M systems although the exact composition boundaries will be system dependent.

Conclusion

The stability of micelles formed from a mixture of a neutral-positively charged diblock copolymer and a metallo-supramolecular polymer was investigated at different polymer and salt concentrations. Dilution of the micellar solutions at constant salt concentrations only decreases the number of micelles but does not change the micellar size. In the presence of 20 mM PIPES buffer, the micelles are stable down to a concentration as low as 0.03 mM. Increasing the salt concentration results in an increase of the CMC, a decrease of the aggregation number, and swelling of the micellar core. The decrease of the aggregation number upon addition of salt is due to the shielding of charges of the ionic blocks that form the micellar core. Micelles are present until a critical salt concentration is achieved. The critical micellar concentration is exponentially dependent on the added salt concentration.

Acknowledgment. The authors thank Dr. A. T. M. Marcelis (Laboratory of Organic Chemistry, Wageningen University, Dreijenplein 8, 6703 HB Wageningen, The Netherlands) for help with the synthesis of L_2EO_4 bisligands. Financial support is from the EU POLYAMPHI/Marie Curie program (RT6-2002, proposal 505027) and SONS Eurocores program (Project JA016-SONS-AMPHI). M. Drechsler gratefully acknowledges financial support by the Deutsche Forschungsgemeinschaft (SFB 481).

References and Notes

(1) Harada, A.; Kataoka, K. *Macromol. Symp.* **2001**, *172*, 1.
(2) Harada-Shiba, M.; Yamauchi, K.; Harada, A.; Takamisawa, I.; Shimokado, K.; Kataoka, K. *Gene Ther.* **2002**, *9*, 407.
(3) Oh, K. T.; Bronich, T. K.; Bromberg, L.; Hatton, T. A.; Kabanov, A. V. *J. Controlled Release* **2006**, *115*, 9.
(4) Cohen Stuart, M. A.; Hofs, B.; Voets, I. K.; de Keizer, A. *Curr. Opin. Colloid Interface Sci.* **2005**, *10*, 30.
(5) Voets, I. K.; de Keizer, A.; de Waard, P.; Frederik, P. M.; Bomans, P. H. H.; Schmalz, H.; Walther, A.; King, S. M.; Leermakers, F. A. M.; Cohen Stuart, M. A. *Angew. Chem. Int. Ed.* **2006**, *45*, 6673.
(6) Cohen Stuart, M. A.; Besseling, N. A. M.; Fokkink, R. G. *Langmuir* **1998**, *14*, 6846.
(7) Van der Burgh, S.; de Keizer, A.; Cohen Stuart, M. A. *Langmuir* **2004**, *20*, 1073.
(8) Hofs, B.; Voets, I. K.; de Keizer, A.; Cohen Stuart, M. A. *Phys. Chem. Chem. Phys.* **2006**, *8*, 4242.
(9) Scholz, C.; Iijima, M.; Nagasaki, Y.; Kataoka, K. *Macromolecules* **1995**, *28*, 7295.
(10) Harada, A.; Kataoka, K. *Science* **1999**, *283*, 65.
(11) Kabanov, A. V.; Kabanov, V. A. *Adv. Drug Delivery Rev.* **1998**, *30*, 49.
(12) Harada, A.; Kataoka, K. *Macromolecules* **1998**, *31*, 288.
(13) Lee, Y.; Fukushima, S.; Bae, Y.; Hiki, S.; Ishii, T.; Kataoka, K. *J. Am. Chem. Soc.* **2007**, *129*, 5362.
(14) Berret, J.-F. *J. Chem. Phys.* **2005**, *123*, 164703.
(15) Berret, J.-F.; Schonbeck, N.; Gazeau, F.; El Kharrat, D.; Sandre, O.; Vacher, A.; Airiau, M. *J. Am. Chem. Soc.* **2006**, *128*, 1755–1761.
(16) Yan, Y.; Besseling, N. A. M.; de Keizer, A.; Marcelis, A. T. M.; Drechsler, M.; Cohen Stuart, M. A. *Angew. Chem. Int. Ed.* **2007**, *46*, 1807.
(17) Yan, Y.; Besseling, N. A. M.; de Keizer, A.; Drechsler, M.; Cohen Stuart, M. A. *J. Phys. Chem. B* **2007**, *111*, 5811.
(18) Vermonden, T.; van der Gucht, J.; de Waard, P.; Marcelis, A. T. M.; Besseling, N. A. M.; Sudholter, E. J. R.; Fleer, G. J.; Cohen Stuart, M. A. *Macromolecules* **2003**, *36*, 7035.
(19) Voets, I. K.; van der Burgh, S.; Farago, B.; Fokkink, R.; Kovacevic, D.; Hellweg, T.; de Keizer, A.; Cohen Stuart, M. A. *Macromolecules* **2007**, *40*, 8476.
(20) Kabanov, A. V.; Bronich, T. K.; Kabanov, V. A.; Yu, K.; Eisenberg, A. *Macromolecules* **1996**, *29*, 6797.
(21) Yuan, X. F.; Harada, A.; Yamasaki, Y.; Kataoka, K. *Langmuir* **2005**, *21*, 2668.
(22) Jaturanpinyo, M.; Harada, A.; Yuan, X. F.; Kataoka, K. *Bioconjugate Chem.* **2004**, *15*, 344.
(23) Yan, Y.; Besseling, N. A. M.; de Keizer, A.; Drechsler, M.; Cohen Stuart, M. A. *J. Phys. Chem. B* **2007**, *111*, 11662.
(24) Biesalski, M. J., D.; Rühe, J. *J. Chem. Phys.* **2004**, *120*, 8807.
(25) Biesalski, M. R. J. *Macromolecules* **1999**, *32*, 2309.
(26) Vermonden, T.; Branowska, D.; Marcelis, A. T. M.; Sudholter, E. J. R. *Tetrahedron* **2003**, *59*, 5039.
(27) Harada, A.; Kataoka, K. *Macromolecules* **2003**, *36*, 4995.
(28) Harada, A.; Kataoka, K. *Langmuir* **1999**, *15*, 4208.
(29) Kramarenko, E. Y.; Khokhlov, A. R.; Reineker, P. *J. Chem. Phys.* **2006**, *125*, 194902.
(30) Solomatin, S. V.; Bronich, T. K.; Bargar, T. W.; Eisenberg, A.; Kabanov, V. A.; Kabanov, A. V. *Langmuir* **2003**, *19*, 8069.
(31) Israelachvili, J. N.; Mitchell, D. J.; Ninhem, B. W. *J. Chem. Soc., Faraday Trans. 2* **1976**, *72*, 1525.
(32) Yan, Y.; Xiong, W.; Li, X. X.; Lu, T.; Huang, J. B.; Li, Z. C.; Fu, H. L. *J. Phys. Chem. B* **2007**, *111*, 22250.
(33) Nagarajan, R. *Langmuir* **2002**, *18*, 31.

JP8044059